TECHNICAL REPORT RD-RE-88-2

EVALUATION OF MULTI-FOCUS HOLOGRAPHIC LENSES

Don A. Gregory
Research Directorate
Research, Development, and
Engineering Center

and

James F. Hawk
University of Alabama at Birmingham
Physics Department
Birmingham, AL

MAY 1988

U.S. ARMY MISSILE COMMAND
Redstone Arsenal, Alabama 35898-5000

Cleared for public release; distribution is unlimited.

UNCLASSIFIED
SECURITY CLASSIFICATION OF THIS PAGE

AD-A196 167

REPORT DOCUMENTATION PAGE

Form Approved
OMB No 0704-0188
Exp Date Jun 30 1986

1a REPORT SECURITY CLASSIFICATION UNCLASSIFIED	1b RESTRICTIVE MARKINGS
2a SECURITY CLASSIFICATION AUTHORITY	3 DISTRIBUTION / AVAILABILITY OF REPORT Cleared for public release; distribution is unlimited.
2b DECLASSIFICATION / DOWNGRADING SCHEDULE	
4 PERFORMING ORGANIZATION REPORT NUMBER(S) TR-RD-RE-88-2	5 MONITORING ORGANIZATION REPORT NUMBER(S)
6a NAME OF PERFORMING ORGANIZATION Research Directorate RD&E Center 6b OFFICE SYMBOL (*If applicable*) AMSMI-RD-RE	7a NAME OF MONITORING ORGANIZATION
6c ADDRESS (*City, State, and ZIP Code*) Redstone Arsenal, AL 35898-5248	7b ADDRESS (*City, State, and ZIP Code*)
8a NAME OF FUNDING / SPONSORING ORGANIZATION 8b OFFICE SYMBOL (*If applicable*)	9 PROCUREMENT INSTRUMENT IDENTIFICATION NUMBER
8c ADDRESS (*City, State, and ZIP Code*)	10 SOURCE OF FUNDING NUMBERS PROGRAM ELEMENT NO. / PROJECT NO / TASK NO / WORK UNIT ACCESSION NO

11 TITLE (*Include Security Classification*)
EVALUATION OF MULTI-FOCUS HOLOGRAPHIC LENSES

12 PERSONAL AUTHOR(S)
Don A. Gregory and James F. Hawk

13a TYPE OF REPORT	13b TIME COVERED	14 DATE OF REPORT (*Year, Month, Day*)	15 PAGE COUNT
Final	FROM _____ TO _____	1988/May/24	23

16 SUPPLEMENTARY NOTATION

17 COSATI CODES			18 SUBJECT TERMS (*Continue on reverse if necessary and identify by block number*)
FIELD	GROUP	SUB-GROUP	hololenses, optical correlator, matched filters,

19 ABSTRACT (*Continue on reverse if necessary and identify by block number*)

The properties of two, 7x7 dichromated gelatin hololenses were measured and compared with the specifications under which they were procured. The intended use for these lenses is a coherent optical correlator. The 49 memory locations would exceed the previously achieved 25 locations and expand the usefulness of the correlator. Several preliminary hololenses were also evaluated which had been made from a new photopolymer from Polaroid, designated DMP-128. Results obtained include the overall diffraction efficiency and the uniformity of the arrays.

20 DISTRIBUTION / AVAILABILITY OF ABSTRACT	21 ABSTRACT SECURITY CLASSIFICATION	
☐ UNCLASSIFIED/UNLIMITED ☒ SAME AS RPT. ☐ DTIC USERS	UNCLASSIFIED	
22a NAME OF RESPONSIBLE INDIVIDUAL Don A. Gregory	22b TELEPHONE (*Include Area Code*) 205-876-7687	22c OFFICE SYMBOL AMSMI-RD-RE

DD FORM 1473, 84 MAR 83 APR edition may be used until exhausted. All other editions are obsolete

SECURITY CLASSIFICATION OF THIS PAGE

CONTENTS

LIST OF ILLUSTRATIONS

LIST OF TABLES

I. INTRODUCTION

An optical correlator using matched filters in a VanderLugt arrangement has been demonstrated to be useful for target discrimination and tracking.[1] Since the Fourier transform is not invariant to rotation and magnification (scale change), an optical correlator, useful for target discrimination and tracking, must contain within its memory (the matched filter/s) a very large number of target pictures from many different orientations and at many different magnifications. One method of making and addressing multiple matched filters in an optical correlator is the hololens developed by Liu and Duthie[2]. Gregory[3] tested a 5x5 hololens produced by Liu and showed that it was possible, using triple exposures of each of the 25 Fourier transforms, to address 73 matched filters in real time. The weak elements in the hololens array were found to correspond to the weak (or the missing two) correlations. Thus, as would be expected, the general quality of the hololens is extremely important in the optical storage and retrieval.

H. K. Liu of LUMIN, Inc. produced and delivered to the Research Directorate in December 1984, two examples of a 7x7 hololens. This hololens almost doubles the potential storage capacity of the 5x5 hololens mentioned above. The purpose of this research was to test the 7x7 hololenses in order to determine their suitability for use in an optical correlator.

Recently, the Research Directorate received samples of a new phase recording media - DMP 128 developed by Polaroid Corporation. This material appears to have several advantages over dichromated gelatin, most notable of which is a greater diffraction efficiency. Several preliminary samples of DMP 128 hololenses were available for comparison with the LUMIN hololenses produced by H. K. Liu.

II. TECHNICAL DISCUSSION

A. Experimental Arrangement

The experimental arrangement for all measurements is shown in Figure 1. An Aerotech 15 mw He/Ne laser was spatially filtered using a 10 micron aperture at the focal point of a 20/0.4 microscope objective. A 390 mm focal length, 55 mm diameter, cemented doublet yielded a reasonably uniform, collimated beam about 50 mm in diameter. The hololenses were located approximately one focal length behind the collimating lens and a variable diaphragm between the two was used to limit the beam diameter to less than the diameter of the hololenses. The screen/photoplate holder could be moved to any position along the optic axis (z direction) and fine screws allowed adjustment in the horizontal (x direction) and vertical (y direction) over a range of 20 mm. An electronic shutter allowed timing for photographs.

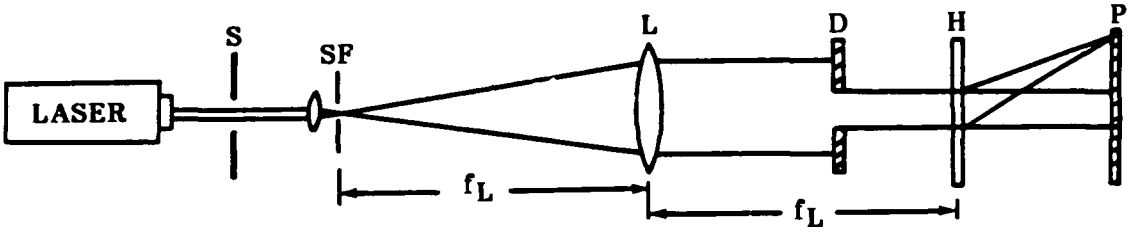

Figure 1. Experimental arrangement: S = shutter, SF = spatial filter, L = collimating lens, D = diaphragm, H = hololens, P = photoplate or screen.

The LUMIN dichromated gelatin hololenses were stored in a dessicator when not in use and the temperature and relative humidity of the laboratory were recorded on each day that testing was done.

B. Focal Length (f_H)

The focal length of each hololens was measured at least three times on separate days. A Ronchi ruling of 4.05 lines per millimeter was placed in the collimated beam just in front of the hololens. The Fourier transform, formed in the focal plane of the hololens, consisted of three bright dots (n = 0, ±1) plus much weaker higher orders. The screen was moved back and

forth until the Fourier transform at each of the 7x7 positions appeared as three, very discreet, dots when viewed through a magnifying glass.

C. Image Diffraction Angle (θ) and Element Spacing (a_H)

With a diameter of 10 mm, the incident beam filled a reasonable portion of the LUMIN hololenses and yielded a very small Airy disc pattern (theoretical first minimum = 1.5 micron) at the focal point. Thus, each Fourier transform in the focal plane consisted of a tiny dot. The main beam (n = 0) and the first diffraction maximum (n = 1), consisting of at least 7x7 elements, was recorded on 4x5 Kodak type 649F photographic plates in the focal plane. The image spacings (a_H) and the distance between the center of the main beam and the center of the 7x7 array (x) were measured on the developed photographic plate. The diffraction angle was calculated from

$$\theta = \tan^{-1} (x/f_H) \quad .$$

Since the image spacing is uniform, the measured image spacing is the average over 8 or 10 elements. These measurements were made with the serial numbered surface facing both toward and away from the incident beam, and the two measurements agreed within experimental error.

D. Diffraction Efficiency

Calling the main beam n = 0 and the 7x7 array n = +1, with the laboratory darkened it was possible to see and measure the n = 0, ±1, and +2 diffraction orders for each LUMIN hololens. A Newport Model 815 Power Meter calibrated at 633 nm was used for all power measurements. The diameter of the Model 815 photodetector is 10 mm, the same as the diameter of the incident beam. With the detector located about 80 mm behind the hololens, the n = ±1 and +2 beams filled the detector. The diffraction efficiency of any order is defined as the power diffracted into that order divided by the incident power (hololens removed from the incident beam) expressed as a percentage. Since the n = +2 order contained less than one percent of the incident power, it may be assumed that any power not diffracted into the n = 0, ±1, +2 is either reflected or absorbed by the hololens. Thus, the incident power absorbed/reflected is obtained by summing the power diffracted into the four orders and dividing by the incident power. It is detailed in the next section, but should be noted here, that a very significant portion of the power diffracted into the n = +1 order lies in elements outside the 7x7 array.

As may be seen from the data in Section III of this report, the diffraction efficiency of the two hololenses is quite different. S/N 04983-1 has a low efficiency, comparable to the 5x5 hololens tested by Gregory[3], while S/N 04983-7 has about three times that efficiency. Diffraction efficiencies were measured with the hololens serial numbers both toward and away from the incident beam. These measurements, however, were not significantly different.

E. Power Distribution Among the Orders

Power distribution among the orders was measured with the Model 815 photodetector covered by an opaque mask with a 0.85 mm hole drilled in the center. The masked detector was taped to a glass plate which could be moved in the x and y directions of the focal plane over the travel of the fine pitch screw (about 20 mm). Absolute power readings were obtained by moving the detector in the x-y plane until a maximum reading on the power meter was obtained. The repeatability of these readings was checked several times before, during, and after recording. Power readings were extended beyond the 7x7 array where possible to indicate the large amount of power contained in elements outside the 7x7 array. The absolute power readings were then divided by the maximum reading (the center or 4/4 element in all cases) and multiplying by 100 to obtain the normalized power readings displayed in Tables 1 through 4 of Section III. Power readings were made with the S/N facing both toward and away from the incident beam.

When comparing the data of Table 1 with Table 2 it is important to realize that the tables show elements in their proper orientation from the viewpoint of the incident beam. When the hololens is turned 180 degrees about the Z axis, the main array (n = +1) goes from left to right. Thus, for example, the second row second column element in Table 1 should correspond most closely with the second row fifth column element of Table 2. The fact that this agreement is not exact may be due, in part, to the angular dependence noted in the next section. $\bar{P}$ is the average normalized power over the 7x7 array only, and σ is the standard deviation.

The data in Tables 1 through 4, when compared with Gregory's[3] Table 3, indicate that the 7x7 hololens has nowhere near the uniformity of the 5x5 hololens. In fact, the weakest elements in the 5x5 hololens have a normalized power almost double the average normalized power of the 7x7 hololens. It is certainly interesting that the average normalized power ($\bar{P}$) and the standard deviation (σ) are almost equal for both 7x7 hololenses. Tables 1 and 2 also indicate why hololens S/N 04983-1 appeared visually to be an 8x8 or 9x9 hololens. Many of the elements outside the 7x7 are hardly diminished from their nearest neighbors.

F. Angular Dependence

LUMIN hololens S/N 04983-7 exhibited an interesting angular dependence which was not apparent with S/N 04983-1. As the hololens was rotated about the y axis, the intensity of the elements in the array varied considerably. This intensity variation was found to be different depending on the orientation of the hololens relative to the incident beam. Since the position of the array in the x - y plane was constant as the hololens was rotated about the y axis, it was possible to make power measurements as a function of angle.

The Model 815 photodiode was positioned in the focal plane such that its 1 cm diameter active portion contained approximately 19 of the elements in the center of the 7x7 array. The hololens was then rotated about the y axis and power was recorded at one-degree increments. This was done with the S/N facing both toward and away from the incident beam (see Figures 2 and 3). In Figures 2 and 3, zero degrees corresponds to the plane of the hololens normal to the incident beam.

TABLE 1. Normalized Power Distribution Among the Elements of LUMIN HOLOLENS S/N 04983-1 with S/N Toward the Incident Beam. P = 20.2 mw, σ = 17.8 mw

1.7	6.5	20.0	14.0	28.5	12.3	13.6	8.5	2.6
3.0	10.2	28.9	16.6	40.4	10.2	12.8	7.7	4.7
3.8	12.8	17.4	28.5	41.7	23.0	8.9	6.0	5.5
5.1	21.3	38.3	16.2	100	40.0	34.1	11.1	6.0
4.3	13.6	16.6	15.7	40.9	25.1	11.1	6.0	5.1
3.8	11.9	28.9	16.2	38.3	11.1	17.0	7.7	5.5
2.6	8.9	20.0	6.8	29.4	11.5	13.2	10.2	3.0
0.9	2.1	4.7	5.5	11.1	6.8	5.1	2.1	1.3

TABLE 2. Normalized Power Distribution Among the Elements of LUMIN HOLOLENS S/N 04983-1 with S/N Away From the Incident Beam P = 20.5 mw, σ = 17.8 mw

0.4	1.7	2.5	4.6	2.9	2.1	0.8	0.4	0.4
0.4	3.4	6.3	9.2	22.3	13.9	13.0	4.2	0.4
0.8	3.8	10.5	16.0	42.9	22.7	23.9	8.0	0.8
1.3	3.8	12.6	22.7	55.9	25.2	23.9	10.9	1.7
1.3	6.3	26.9	42.0	100	44.5	41.6	18.1	2.5
1.7	4.2	14.3	23.5	55.0	26.5	25.6	11.3	1.7
0.8	3.8	12.2	16.8	41.6	24.8	25.2	8.8	1.7
0.4	3.4	3.4	5.9	10.1	24.4	15.1	13.9	5.9
0.4	0.8	2.1	3.4	5.0	3.4	2.5	0.8	0.8

TABLE 3. Normalized Power Distribution Among the Elements of LUMIN HOLOLENS S/N 04983-7 With S/N Toward the Incident Beam P = 18.9 mw, σ = 16.3 mw

0.7	1.0	1.5	1.8	4.0	2.5	1.8	0.9	0.4
1.3	5.1	11.7	16.2	30.7	12.0	9.4	2.8	1.2
2.2	8.4	12.1	12.3	28.2	12.7	12.1	7.5	1.5
1.2	12.7	9.6	21.3	51.4	18.1	14.1	11.8	1.6
1.9	18.0	16.3	45.6	100	38.4	24.9	21.3	2.8
1.5	14.7	10.3	21.6	52.3	18.6	15.3	12.0	1.3
2.2	9.0	13.0	13.8	30.3	14.2	13.0	7.2	1.3
1.3	5.7	11.8	17.1	38.4	12.6	8.1	3.1	1.2
0.6	0.9	1.2	1.9	4.5	1.8	1.3	0.9	0.3

TABLE 4. Normalized Power Distribution Among the Elements of LUMIN HOLOLENS S/N 04983-7 With S/N Away From the Incident Beam P = 18.2 mw, σ = 16.0 mw

0.8	3.2	9.9	11.8	27.7	15.7	12.3	4.4
1.0	7.3	9.8	11.1	25.3	9.6	10.1	8.6
1.3	11.8	11.1	17.0	50.1	17.5	8.1	13.5
2.4	19.9	18.2	37.4	100	40.6	16.6	18.4
1.2	13.2	13.1	17.8	50.5	18.5	9.8	16.7
1.2	7.9	12.6	14.1	27.4	13.0	13.6	11.5
1.0	3.9	9.9	14.2	39.0	19.6	14.1	6.1

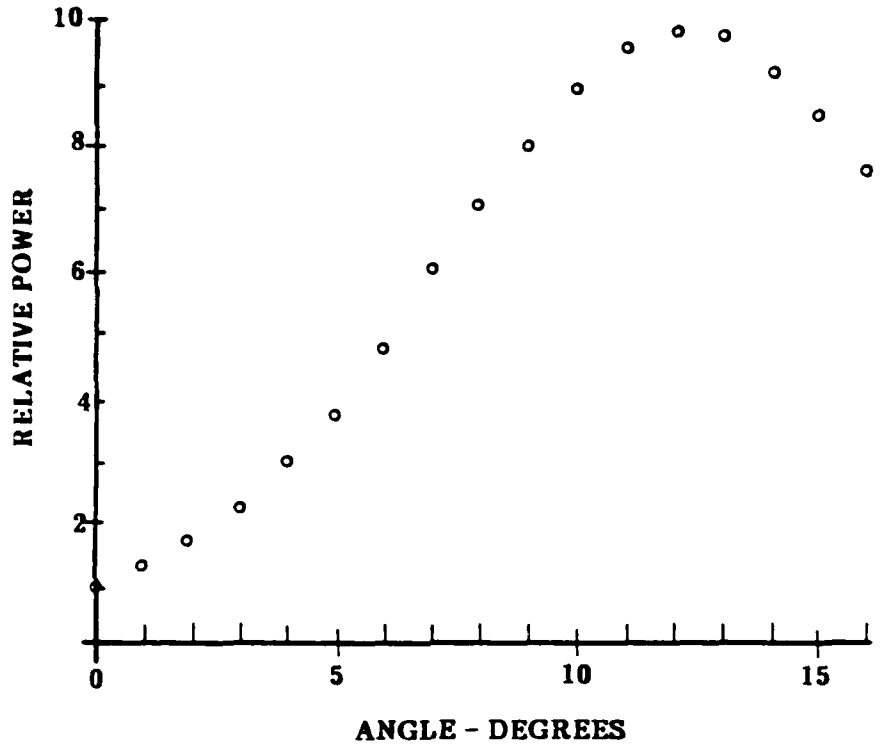

Figure 2. Variation of power with angle hololens S/N 04983-7 - S/N away from incident beam.

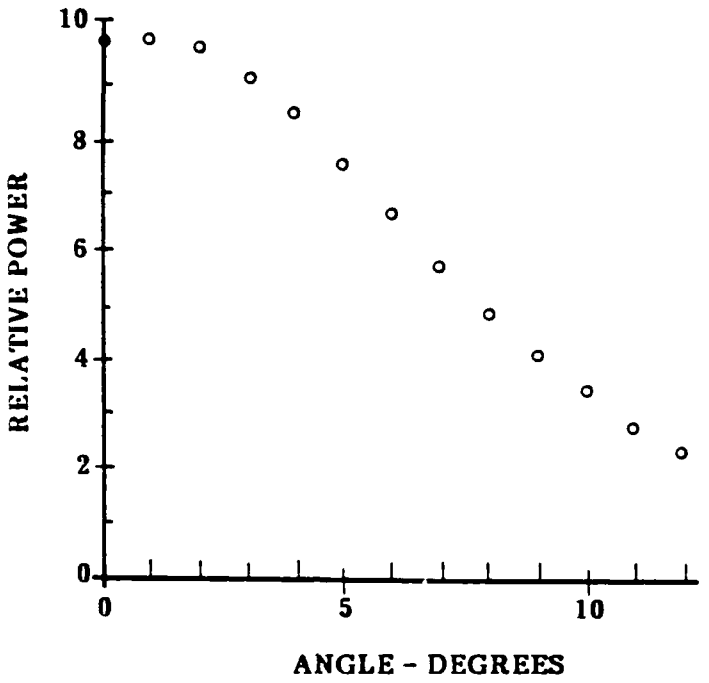

Figure 3. Variation of power with angle hololens S/N 04983-7 with S/N toward incident beam.

It is interesting to note that, with the S/N turned away from the incident beam, maximum power was recorded at slightly greater than 12 degrees, which agrees quite well with the measured diffraction angle for that hololens. However, with the S/N turned toward the incident beam, the maximum power was observed when the hololens was normal to the incident beam.

G. Image Quality

Quantitative measurements of image quality, such as modulation transfer function or point spread, were not done in this research, but some qualitative observations help to indicate the utility of the holographic lenses as elements in an optical correlator. A black 35 mm slide with 6 small, circular openings arranged in a hexagonal pattern was placed in front of the hololenses. The 7x7 array of images were recorded on 649 F plates placed just beyond the focal point. These images, though varying greatly in intensity, appeared to be of the same quality as those formed by a double convex lens of the same focal length and diameter as the hololens. In addition, the Fourier transform of the 4.05 lines per mm Ronchi ruling, which was used to accurately determine the focal point, consisted of very discreet dots about one-half millimeter apart as would be predicted theoretically.

It would appear that the main problem in using these hololenses as part of an optical correlator would be the same ones encountered using the 5x5 hololens - the fact that the image brightness varies so greatly from element to element.

H. DMP 128 Measurements

Only one of the DMP 128 holographic elements evaluated was actually a hololens. The others were simple diffraction gratings. Measurements of focal length, diffraction angle, and diffraction efficiency were made in the same fashion as described for the LUMIN hololenses. For the other four elements, only diffraction efficiencies and angles were measured.

III. EXPERIMENTAL RESULTS

A. Manufacturer's Specifications - LUMIN Hololens S/N 04983-1

LUMIN	7x7
MODEL - 049	f_H = 29 cm
SERIAL - 04983-1	a_H = 2.5 mm
HOLOLENS	θ = 8°

B. Measured Values - LUMIN Hololens S/N 04983-7

f_H = 21.3 ± 0.3 cm	Mounting 66 mm x 87 mm
a_H = 2.52 ± 0.02 mm	metal frame
θ = 9.6° ± 0.5°	Diameter = 18.0 mm

Incident Power Absorbed/Reflected 19.8 ± 0.8%

Diffraction Efficiency

S/N Toward Incident Beam	8.2%	(n = +1)
	2.7%	(n = -1)
S/N Away From Incident Beam	6.0%	(n = +1)
	4.6%	(n = -1)

Diffraction into n = +2 order, less than 1%

C. Manufacturer's Specifications - DMP 128 Hololens

LUMIN	7x7
MODEL - 049	f_H = 27 cm
SERIAL - 04983-7	a_H = 2.5 mm
HOLOLENS	θ = 10°

D. Measured Values - DMP 128 Diffraction Screen

f_H = 20.2 ± 0.2 cm Mounting 51 mm x 61 mm

a_H = 2.52 ± 0.02 mm metal frame

θ = 13.1° ± 0.3° Diameter = 18.5 mm

Incident Power Absorbed/Reflected	16.5 ± 0.5%
Diffraction Efficiency	
S/N Toward Incident Beam	22.8% (n = +1)
	1.4% (n = -1)

diffraction into n = +2 order less than 1%
S/N Away From Incident beam not measured because of strong angular dependence.

E. DMP 128 Hololens - no identification number

measured values

f_H = 24 cm Mounting 5 cm x 5 cm glass plate

a_H = 3.5 mm

θ = 17° Diameter 5 mm

Incident Power Absorbed/Reflected 14%

Diffraction Efficiency 7% (n = +1)
3% (n = -1)

This hololens is strongest in the 3x3 array but it is fairly strong in 5x5 and moderately strong in 6x6.

F. DMP 128 Diffraction Screen - ID # 4-29-86-1

measured values Mounting 5 cm x 5 cm glass plate

f_H = none Diameter = 5 mm

Immediately behind the diffraction screen the 5 mm diameter laser beam is diffracted into four orders: n = +2, +1, 0, and -1. The n = 2 looks like a 3x3 array of dots which seem to be sharpest at about 2 cm. The n = +1 looks like a 3x3 array, much more intense than the n = +2, with moderately intense 5x5. The n = +1 is sharpest at about 3.5 cm. Diffraction efficiency of n = +1 is 27%. The elements of these arrays are unaffected, except in intensity, by insertion of the Ronchi ruling. The n = 0 and n = -1 are not divided into elements. Diffraction efficiency of n = 0 is 33% and the diffraction efficiency of n = -1 is 11%.

G. Three DMP Diffraction Gratings - ID # 46

measured values

f_H = none Mounting 5 cm x 5 cm glass plate

Diameter 9 mm

All three gratings behave more or less the same. They absorb/reflect about 28% of the incident power and diffract the beam into four orders with angles and diffraction efficiencies listed below:

(n = -1)	θ = -20°	6%
(n = 0)	θ = 0°	15%
(n = +1)	θ = +20°	46%
(n = +2)	θ = +42°	4%

These four orders are not divided into arrays of elements nor do they have any focal point.

IV. CONCLUSIONS

The LUMIN hololenses form Fourier Transforms and images of good quality, but the power distribution among elements is extremely non-uniform. The diffraction efficiency of the two lenses tested are quite different, but Hololens S/N 04983-7 shows that hololenses of much greater diffraction efficiency may be made in dichoromated gelatin. The only DMP-128 hololens tested had a very low diffraction efficiency, but some samples of DMP 128 diffraction gratings show that diffraction efficiencies higher than dichromated gelatin are possible.

REFERENCES

1. Farr, K., "Real Time Vehicle Tracking," Research Directorate, U. S. Army Missile Command, Redstone Arsenal, AL (unpublished video tape).

2. Liu, H. K., and Duthie, J. G., Appl. Opt. 21: 3278 (1982).

3. Gregory, D. A., "Real Time Large Memory Optical Pattern Recognition," Technical Report RR-84-9, U.S. Army Missile Command, Redstone Arsenal, AL (June 1984).

DISTRIBUTION

	No. of Copies
Director US Army Research Office ATTN: SLCRO-PH PO Box 12211 Research Triangle Park, NC 27709-2211	1
Director US Army Research Office ATTN: SLCRO-ZC PO Box 12211 Research Triangle Park, NC 27709-2211	1
Headquarters Department of the Army ATTN: DAMA-ARR Washington, DC 20310-0632	1
Headquarters OUSDR&E ATTN: Dr. Ted Berlincourt The Pentagon Washington, DC 20310-0632	1
Defense Advanced Research Projects Agency Defense Sciences Office Electronics Systems Division ATTN: Dr. John Neff 1400 Wilson Boulevard Arlington, VA 22209	1
Commander US Army Foreign Science and Technology Center AIAST-RA 220 Seventh Street Ne Charlottesville, VA 22901-5396	1
Commander US Army Strategic Defense Command DASD-H-V PO Box 1500 Huntsville, AL 35807-3801	1
Director, URI University of Rochester College of Engineering and Applied Science The Institute of Optics Rochester, NY 14627	1

	No. of Copies
Director, JSOP University of Arizona Optical Science Center Tucson, AZ 85721	1
Dr. Steve Butler Electro-Optical Terminal Guidance Branch Armament Laboratory Eglin Air Force Base, FL 32542	1
Dr. Richard Munis US Army CRREL 72 Lyme Mill Rd. Hanover, NH 03755	1
Mark Norton AMSEL-NV-T Night Vision and Electro-Optics Center Bldg 357 Fort Belvoir, VA 22060	1
Dr. Joseph Horner RADC/ESOP Hanscom AFB, MA 01731	1
Dr. Robert D. Buzzard Applied Science Division Applied Optics Operations P.O. Box 3115 Garden Grove, CA 92641	1
Dr. J. W. Goodman Department of Electrical Engineering Stanford University Stanford, CA 94305	1
Dr. H. John Caulfield University of Alabama in Huntsville Center for Applied Optics Huntsville, AL 35899	1
Dr. J. G. Duthie University of Alabama in Huntsville Physics Department Huntsville, AL 35899	1

	No. of Copies
Dr. David Casasent Carnegie-Mellon University Department of Electrical and Computer Engineering Pittsburgh, PA 15213	1
Dr. F. T. S. Yu Penn State University Department of Electrical Engineering University Park, PA 16802	1
Mr. James F. Hawk University of Alabama in Birmingham Physics Department University Station Birmingham, AL 35294	1
Dr. Richard Juday NASA Johnson Space Center Code EE-6 Houston, TX 77058	1
Dr. Michael Shumate Jet Propulsion Lab 4800 Oak Grove Drive Pasadena, CA 91109	1
David Bloom Naval Weapons Center Code 3941 China Lake, CA 93555	1
Dr. Kristina Johnson University of Colorado at Boulder Dept. of Electrical & Computer Engineering Boulder, Colorado 80309-0425	1
Dr. Arthur Fisher Code 6537 Naval Research Lab Washington, DC 20375-5000	1
US Army Materiel System Analysis Activity ATTN: AMXSY-MP Aberdeen Proving Ground, MD 21005	1

DISTRIBUTION (Concluded)

	No. of Copies
IIT Research Institute ATTN: GACIAC 10 W. 35th Street Chicago, IL 60616	1
AMSMI-RD, Dr. McCorkle	1
Dr. Rhoades	1
AMSMI-RD-RE, Dr. J. Bennett	1
AMSMI-RD-RE-OP, Dr. Charles Bowden	1
Dr. Don A. Gregory	50
Mr. David J. Lanteigne	1
Mr. James C. Kirsch	1
Mr. Tracy D. Hudson	1
AMSMI-RD-CS-R	15
AMSMI-RD-CS-T	1
AMSMI-GC-IP, Mr. Bush	1